

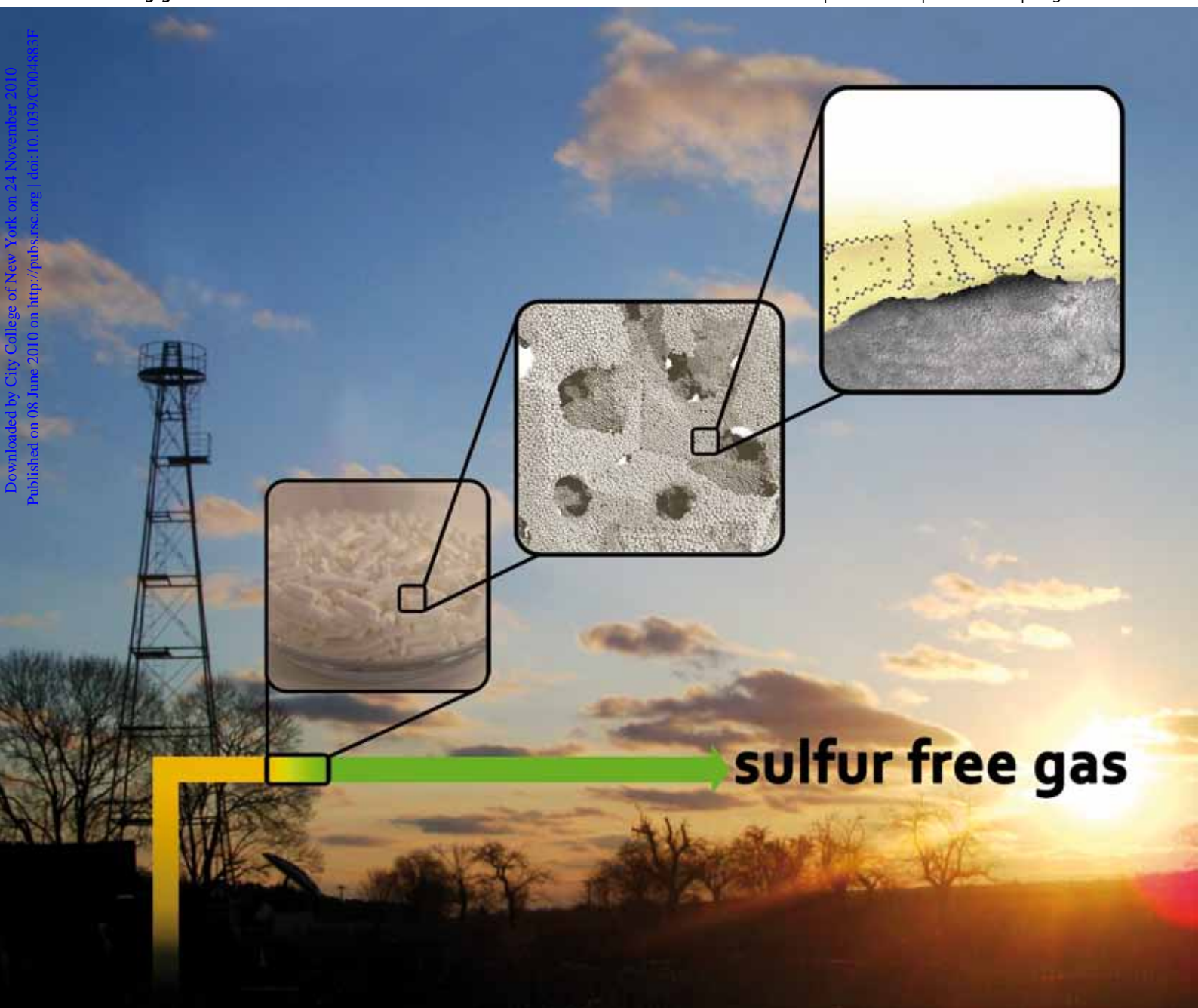
Green Chemistry

Cutting-edge research for a greener sustainable future

www.rsc.org/greenchem

Volume 12 | Number 6 | June 2010 | Pages 925–1112

Downloaded by City College of New York on 24 November 2010
Published on 08 June 2010 on <http://pubs.rsc.org> | doi:10.1039/C004483F



ISSN 1463-9262

RSC Publishing

Haumann and Wasserscheid *et al.*
Continuous gas-phase desulfurisation

Jiménez-Aparicio *et al.*
Microwave synthesis of paddlewheel
compounds

Stolle *et al.*
Sonogashira coupling in a ball mill

Dumesic *et al.*
Hydrocarbon transportation fuels from
biomass

Continuous gas-phase desulfurisation using supported ionic liquid phase (SILP) materials

Florian Kohler, Daniel Roth, Esther Kuhlmann,[†] Peter Wasserscheid* and Marco Haumann*

Received 6th April 2010, Accepted 23rd April 2010

First published as an Advance Article on the web 21st May 2010

DOI: 10.1039/c004883f

Supported ionic liquid phase (SILP) materials have been developed for a continuous gas cleaning process. The technology is exemplified for the desulfurisation of a model gas stream consisting of 500 ppm_w n-butyl mercaptan in n-heptane vapour to levels of mercaptan below 5 ppm_w. By varying the ionic liquid structure, acidity and loading, [C₁₂MIM]Cl/SnCl₂ (X_{SnCl₂} = 0.50) on alumina in an ionic liquid loading of 20 vol% of the support's pore volume was identified as a particularly suitable gas sorption system. Breakthrough experiments demonstrate desulfurisation performance of up to 130 h time-on-stream, and the suitability of the system for loading/unloading cycles in a pressure and temperature swing operation mode.

Introduction

The removal of sulfur compounds from fuels to a level of below 10 ppm saves the environment from SO₂ emissions from the transport sector and is mandatory due to legislative regulations.^{1,2} In today's refineries, this task is usually completed by catalytic hydrodesulfurisation (HDS), where S-containing organic compounds are converted into H₂S and hydrogenated hydrocarbons.³ An interesting alternative to the HDS process that does not require a hydrogen infrastructure and high pressure equipment is the selective extraction of sulfur compounds by an inert, recyclable extraction solvent. For this purpose, the use of ionic liquids has been suggested by us and other research groups, since these ionic media combine an extremely low volatility and high solubility for S-compounds with low to moderate solubilities for saturated hydrocarbons.^{4–10}

In the first application of this alternative desulfurisation technology, Lewis-acidic ionic liquids of the general type [C_nMIM]Cl/AlCl₃ (n = 2, 4; molar excess of AlCl₃) were applied as reactive extraction media to lower the sulfur content of a model oil from 500 ppm_w to less than 10 ppm_w by repetitive extraction in four extraction stages.⁴ Later, neutral ionic liquids such as tetrafluoroborates, hexafluorophosphates, alkylsulfates¹¹ and dialkylphosphates⁹ were successfully applied to extract S-compounds from model oils and real diesel fuel.

It is noteworthy that the development of efficient extractive desulfurisation systems does not only concern the optimisation of the thermodynamic solubility of S-compounds but also the maximisation of the rate of mass transfer. As the latter is often restricted by high ionic liquid viscosity, reaching an equilibrium

composition in ionic liquid–organic biphasic systems often requires extended contact times.

Supported ionic liquid phase (SILP) materials have recently been introduced to overcome this limitation.^{12,13} In SILP materials, a small amount of ionic liquid is dispersed on the internal surface of a porous material, creating a physisorbed thin film in the nm range.

The SILP concept has been successfully applied for the immobilisation of homogeneous transition metal complexes, and many of these materials have demonstrated very interesting performances in gas-phase, fixed-bed, catalytic reactions.^{12,14–18} Recently, the technology has also been tested in the slurry-phase desulfurisation of n-butyl mercaptan from n-heptane. Making use of the high exchange surface and short diffusion distances offered by these materials, a highly efficient absorption/adsorption process could be realised.⁹ Compared to the corresponding bulk ionic extraction, the extraction times with the same chlorometallate ionic liquids could be reduced by factors of up to 50. Note that desulfurisation with SILP materials is macroscopically an adsorption but microscopically an absorption process.

In this work, we demonstrate for the first time the application of SILP materials in a continuous gas cleaning process. To allow the best possible comparison with our former⁹ slurry-phase desulfurisation experiments, we have investigated the selective removal of n-butyl mercaptan vapour from an n-heptane gas phase as an instructive example for this proof-of-principle study. Fig. 1 schematically illustrates the concept of a continuous gas cleaning process using an SILP material in a fixed-bed sorption column.

Experimental

Materials

Zinc(II) chloride (Merck, for analysis), tin(II) chloride (Merck, water-free for synthesis), n-butyl mercaptan (Merck, ≥ 98.0%), n-heptane (Merck, ≥ 99.0%), 1-butyl-3-methylimidazolium

Lehrstuhl für Chemische Reaktionstechnik, Universität Erlangen-Nürnberg, Egerlandstraße 3, 91058, Erlangen, Germany.
E-mail: peter.wasserscheid@crt.cbi.uni-erlangen.de, marco.haumann@crt.cbi.uni-erlangen.de; Fax: +49 9131 85-27421; Tel: +49 9131 85-27429

[†] Current address: Lanxess Deutschland GmbH, Gebäude F 46, 41538, Dormagen, Germany.

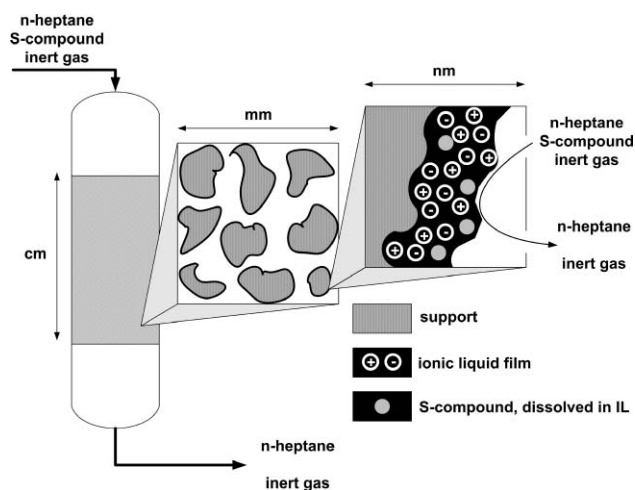


Fig. 1 A schematic illustration of an SILP material applied in a gas purification process using a fixed-bed sorption column.

chloride [C_4MIM]Cl (Merck, $\geq 97.0\%$) and 1-methyl-3-octylimidazolium chloride [C_8MIM]Cl (Fluka, $\geq 97.0\%$) were used as received without any further purification.

1-Dodecyl-3-methylimidazolium chloride [$C_{12}MIM$]Cl and 1-dodecyl-3-methylimidazolium bis[(trifluoromethyl)sulfonyl]-amide [$C_{12}MIM$][Tf_2N] were prepared and purified according to the literature.^{19–21}

The meso-/macroporous alumina support was provided by Sasol Germany GmbH (Al_2O_3 -extrudates, $S_{BET} = 125.1 \text{ m}^2 \text{ g}^{-1}$, $V_{\text{pore}} = 0.611 \text{ cm}^3 \text{ g}^{-1}$) and applied after drying in a vacuum of 4×10^{-4} mbar.

Preparation of the chlorometallate ionic liquids

The chlorometallate ionic liquids applied in this study were synthesized by mixing equimolar amounts of the respective imidazolium chloride salt with zinc(II) chloride or tin(II) chloride at $70 \text{ }^\circ\text{C}$ for 24 h. All operations were carried out under an inert atmosphere using standard Schlenk techniques. After their formation, all of the chlorometallate ionic liquids were dried for 1 h at $60 \text{ }^\circ\text{C}$ under a vacuum of 4×10^{-4} mbar. Chlorometallate ionic liquids of varying Lewis acidity were obtained by mixing [$C_{12}MIM$]Cl/ $SnCl_2$ with different molar ratios (2 : 1, 1 : 1, 1 : 1.3 and 1 : 1.6), resulting in metal contents, X , of $SnCl_2$ of $X = 0.33$, 0.50, 0.57 and 0.62, respectively.

Preparation of SILP materials

All SILP materials were prepared under an inert atmosphere using standard Schlenk techniques. The required amount of chlorometallate ionic liquid (typically 2–5 g) was dissolved in 60 ml dichloromethane (water content < 10 ppm) by stirring the mixture for 20 min. The required amount of support to adjust the desired ionic liquid loading, α , was added to this solution. α of the SILP materials was calculated according to eqn (1).

$$\alpha = \frac{V_{IL}}{m_{\text{support}} V_{\text{pore}}} \left[\frac{m_{IL} g_{\text{support}}}{g_{\text{support}} m_{\text{pore}}} \right] \quad (1)$$

After stirring the ionic liquid–support suspension for 1 h, the solvent was removed and the SILP material dried at $60 \text{ }^\circ\text{C}$ under a 4×10^{-4} mbar vacuum.

SILP materials with two different ionic liquid loadings were prepared, namely 10 and 20 vol%. The specific pore volume and the specific BET surface area of the original support were determined using a Micrometrics ASAP instrument.

Thermogravimetry analysis (TGA)

TGA measurements were carried out using a Netzsch TG 209 F3 Tarsus instrument. 70 mg of SILP material was heated from 30 to $400 \text{ }^\circ\text{C}$ at a heating rate of 10 K min^{-1} . For long-term stability measurements, TGA curves were recorded isothermally at $120 \text{ }^\circ\text{C}$ for 700 min under a 20 mbar vacuum.

SILP absorption measurements

Fig. 2 shows a schematic view of the experimental set-up applied in the here-described SILP gas sorption experiments.

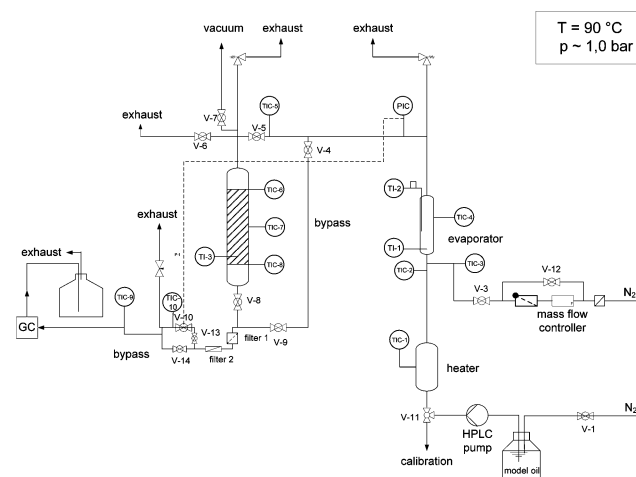


Fig. 2 The experimental set-up applied in the SILP gas sorption experiments of this study.

The applied model oil (MO; 500 ppm_w n-butyl mercaptan in n-heptane) was pumped with a volumetric flow of $V_{MO} = 0.2 \text{ ml min}^{-1}$ using a HPLC pump (Knauer) to an evaporator unit. There, the liquid was evaporated, assisted by a nitrogen flow of $40.0 \text{ Nml min}^{-1}$. In all of the measurements, the obtained vapour mixture (total gas flow rate = 87.5 ml min^{-1}) was passed through a SILP fixed-bed column containing 10.7 g of SILP material corresponding to a bed height of approximately 90 mm in our setup. The sorption temperature was kept constant at $90 \text{ }^\circ\text{C}$ and the sorption column was operated under atmospheric pressure. The amount of n-butyl mercaptan at the column outlet was determined by an online gas chromatograph (Varian CP-3800, HP-FFAP capillary column cross-linked FFAP, $30 \text{ m} \times 0.53 \text{ mm}$). The change of n-butyl mercaptan content was recorded over time. The breakthrough time, t_b , was determined once the first detectable concentration of n-butyl mercaptan had been picked up by the GC (detection limit = 5 ppm_{w}).

During regeneration, the SILP material inside the column was exposed to a vacuum (2.5×10^{-2} mbar) at $130 \text{ }^\circ\text{C}$ for 180 min.

The breakthrough and saturation capacities reflect the absorbed amount of n-butyl mercaptan until breakthrough or

Table 1 The decomposition temperatures of different SILP materials with an ionic liquid pore filling of $\alpha = 20$ vol% on the Al_2O_3 support^a

SILP	Metal content X	$T_{\text{dec}}/^\circ\text{C}$
$[\text{C}_4\text{MIM}]\text{Cl}/\text{ZnCl}_2$	0.50	318.4
$[\text{C}_4\text{MIM}]\text{Cl}/\text{SnCl}_2$	0.50	267.7
$[\text{C}_8\text{MIM}]\text{Cl}/\text{SnCl}_2$	0.50	258.8
$[\text{C}_{12}\text{MIM}]\text{Cl}/\text{SnCl}_2$	0.33	259.3
$[\text{C}_{12}\text{MIM}]\text{Cl}/\text{SnCl}_2$	0.50	265.1
$[\text{C}_{12}\text{MIM}]\text{Cl}/\text{SnCl}_2$	0.57	271.0
$[\text{C}_{12}\text{MIM}]\text{Cl}/\text{SnCl}_2$	0.62	277.3
$[\text{C}_{12}\text{MIM}][\text{TF}_2\text{N}]$	—	326.3

^a Heating rate of the TG apparatus = 10 K min^{-1} in the temperature range 30–400 °C.

saturation ($c = c_0$), respectively. The breakthrough and saturation capacities, x_b and x_s , were calculated according to eqn (2) and eqn (3).

$$x_b = \frac{\dot{m}}{m_{\text{SILP}}} \times t_b \quad (2)$$

$$x_s = \frac{\dot{m}}{m_{\text{SILP}}} \times t_h \quad (3)$$

The half-life time, t_h , is defined as the time when the c/c_0 ratio reaches the value of 0.5.

Results and discussion

Thermal stability

All of the SILP materials were first tested for their thermal stability by thermogravimetric analysis in the temperature range between 30 and 400 °C. For these experiments, the ionic liquid loading was adjusted to 20 vol% pore filling. The results for the $[\text{C}_n\text{MIM}]\text{Cl}/\text{SnCl}_2$ - ($n = 4, 8, 12$), $[\text{C}_4\text{MIM}]\text{Cl}/\text{ZnCl}_2$ - and $[\text{C}_{12}\text{MIM}][\text{TF}_2\text{N}]$ -based SILP materials, as well as the neat Al_2O_3 support (0 vol% ionic liquid), are shown in Fig. 3. The determined decomposition temperatures of the tested SILP materials are summarised in Table 1.

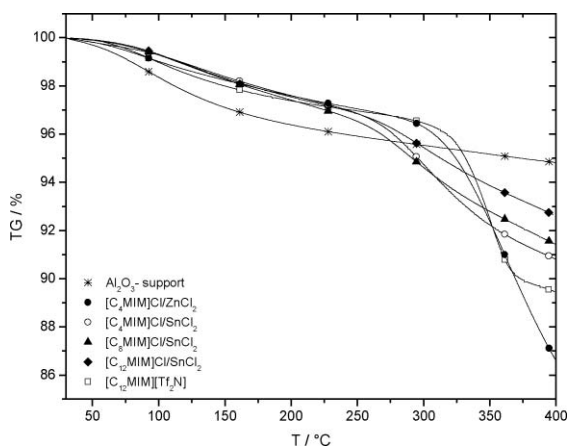


Fig. 3 Thermogravimetric measurements of the neat Al_2O_3 support ($\alpha = 0$ vol%) and SILP materials with a pore filling of $\alpha = 20$ vol% and $X = 0.50$ in case of chlorometallate ionic liquids at a heating rate of the TG apparatus of 10 K min^{-1} in the temperature range 30–400 °C.

For all the materials, a slow mass loss in the range 30–200 °C was observed, attributed to a slow evaporation of water from the alumina support (see also the TGA curve of the pure support). The water range is extended to 200 °C due to the fact that water is both surface bound on the alumina support and interacting with the more or less Lewis acidic ionic liquid. At specific temperatures above 200 °C, thermal decomposition of the different SILP materials is observed. Following the variation of the metal content and Lewis acidity in the $[\text{C}_{12}\text{MIM}]\text{Cl}/\text{SnCl}_2$ -based SILP material series, the decomposition temperature increases from 260 °C ($X = 0.33$) to 277 °C ($X = 0.62$). All the TGA results indicate that the applied ionic liquids should be stable under the conditions of gas-phase desulfurisation at 90 °C.

To also test the stability of the SILP systems under the conditions of regeneration, all of the materials were tested for 700 min at 120 °C under a 20 mbar pressure in the TGA device. No significant mass loss was observed in these experiments.

Ionic liquid variation

Our previous work on the SILP-assisted removal of n-butyl mercaptan from an n-heptane solution by slurry-phase absorption/adsorption indicated that ionic liquids of the type $[\text{C}_4\text{MIM}]\text{Cl}/\text{ZnCl}_2$ and $[\text{C}_4\text{MIM}]\text{Cl}/\text{SnCl}_2$ do not only exhibit good extraction performance for S-compounds, but also allow the reuse of the SILP material for at least five consecutive extractions after thermal regeneration.⁹ The same SILP materials were used as the starting points for the gas-phase desulfurisation studies presented here.

The results of the corresponding breakthrough experiments are presented in Fig. 4. Interestingly, the $[\text{C}_4\text{MIM}]\text{Cl}/\text{ZnCl}_2$ -based SILP system showed the weakest absorption performance, with a breakthrough already after 60 min time-on-stream. In the same time range, effective desulfurisation was also found for the neat alumina support without any ionic liquid loading (see Fig. 6), making a desulfurisation effect by the applied ionic liquid dubious. The best purification performance was obtained for SnCl_2 -based SILP systems, with a clear trend for longer

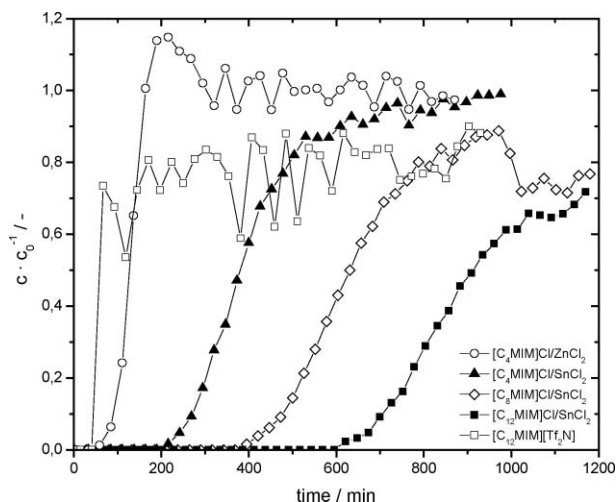


Fig. 4 Normalised breakthrough curves of n-butyl mercaptan recorded for different SILP absorber materials with $X = 0.50$ in case of chlorometallate ionic liquids; $T_{\text{abs}} \sim 90$ °C, $p = 1.05$ bar, $m_{\text{SILP}} = 10.6$ g, $h \sim 90$ mm, $V_{\text{N}_2} = 40 \text{ Nml min}^{-1}$, $V_{\text{MO}} = 0.2 \text{ ml min}^{-1}$.

breakthrough times (*i.e.* better desulfurisation performance) with increasing lipophilicity of the ionic liquid's cation.

The $[\text{C}_4\text{MIM}]\text{Cl}/\text{SnCl}_2$ -based SILP material could retain 100% n-butyl mercaptan for 200 min, whereas the SILP materials based on $[\text{C}_8\text{MIM}]\text{Cl}/\text{SnCl}_2$ and $[\text{C}_{12}\text{MIM}]\text{Cl}/\text{SnCl}_2$ gave 100% removal for 380 and 600 min, respectively. The positive effect of the longer alkyl chains at the imidazolium cation on the desulfurisation performance is attributed to the lower packing density of ions in these systems, creating more space for the S-containing solute within the ionic liquid. A positive influence of longer chain-substituted imidazolium ions on the solubility of S-compounds in ionic liquids was also reported for the case of a liquid–liquid extraction in the recent literature.²² While, in the latter case, the higher viscosity of long chain-substituted imidazolium salts can easily harm the overall extraction performance due to slow mass transfer, the SILP concept, with its characteristic diffusion lengths in the nm range, allows full benefit to be taken of this solubility advantage. This exemplifies impressively the beneficial effect of SILP technology for the application of relatively viscous ionic liquids in a continuous gas cleaning process.

Using $[\text{C}_{12}\text{MIM}][\text{Tf}_2\text{N}]$ coated onto alumina, the breakthrough time was found to be reduced to less than 60 min, highlighting the importance of the weak chemisorptive effect of the Lewis acidic nature of the ionic liquids' anion in the case of chlorostannate ionic liquids. Remarkably, this value is also lower than the one found for the neat support, indicating that the hydrophobic ionic liquid takes away pore volume and surface area of the support that could otherwise accommodate the adsorbed n-butyl mercaptan. Due to the findings of this ionic liquid variation study, all further experiments were carried out with $[\text{C}_{12}\text{MIM}]\text{Cl}/\text{SnCl}_2$ -based SILP materials.

Variation of the ionic liquid's Lewis acidity for chlorostannate-based SILP materials

The molar ratio, X , of SnCl_2 in the ionic liquid $[\text{C}_{12}\text{MIM}]\text{Cl}/\text{SnCl}_2$ was varied systematically from $X = 0.33$ (Lewis-basic ionic liquid) to $X = 0.62$ (Lewis-acidic ionic liquid). In Fig. 5, the results of the corresponding continuous absorption experiments of n-butyl mercaptan are summarised.

The basic ionic liquid $[\text{C}_{12}\text{MIM}]\text{Cl}/\text{SnCl}_2$ ($X = 0.33$) gave unsatisfying results, with n-butyl mercaptan breakthrough after only 150 min time-on-stream. The fact that, after breakthrough, c/c_0 values of slightly higher than 1.0 were observed can be explained by the known effect of n-butyl mercaptan accumulation on the fixed-bed during absorption.²³ As already shown in Fig. 4, the use of the neutral ionic liquid $[\text{C}_{12}\text{MIM}]\text{Cl}/\text{SnCl}_2$ ($X = 0.50$) yielded a significantly extended breakthrough time of 620 min. Surprisingly, a further increase of the metal content to $X = 0.57$ and 0.62 resulted in Lewis-acidic SILP systems that did not show a higher sorption capacity for n-butyl mercaptan, despite the increase in coordinating metal species.

The results from the ionic liquid and metal variation experiments are summarised in Table 2.† The best saturation

† Values for the pure ionic liquid could not be determined since the thermodynamic equilibrium was not adjusted, even after 30 h stirring, due to the high viscosity of the ionic liquids applied. See also Ref. 9.

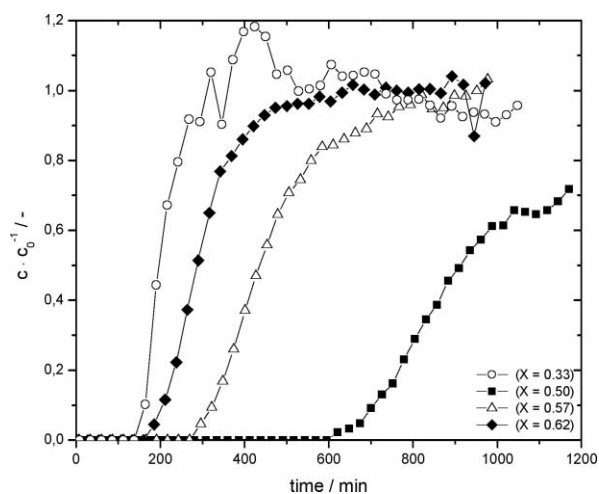


Fig. 5 Normalised breakthrough curves of n-butyl mercaptan with $[\text{C}_{12}\text{MIM}]\text{Cl}/\text{SnCl}_2$ -based SILP materials ($\alpha = 20$ vol%) of different Lewis acidity; $T_{\text{abs}} \sim 90$ °C, $p = 1.05$ bar, $m_{\text{SILP}} = 10.6$ g, $h \sim 90$ mm, $V_{\text{N}_2} = 40$ Nml min^{-1} , $V_{\text{MO}} = 0.2$ ml min^{-1} .

and breakthrough capacities, x_s and x_b , were found for the $[\text{C}_{12}\text{MIM}]\text{Cl}/\text{SnCl}_2$ loading, with $x_s = 5.76$ $\text{mg}_s \text{g}_{\text{SILP}}^{-1}$ and $x_b = 3.90$ $\text{mg}_s \text{g}_{\text{SILP}}^{-1}$.

One possible explanation for the reduced extraction capability of acidic stannate melts might be the formation of the dimeric and trimeric stannate ions $[\text{Sn}_2\text{Cl}_5]^-$ and $[\text{Sn}_3\text{Cl}_8]^-$, reducing the concentration of $[\text{SnCl}_3]^-$, which obviously shows the highest potential for the chemisorptive binding of n-butyl mercaptan to the SILP material.

Ionic liquid loading variation

The loading of the ionic liquid $[\text{C}_{12}\text{MIM}]\text{Cl}/\text{SnCl}_2$ ($X = 0.50$) on alumina was varied between $\alpha = 0$ (no ionic liquid coating on support) and $\alpha = 20$ vol%. The results of the corresponding sorption studies are depicted in Fig. 6.

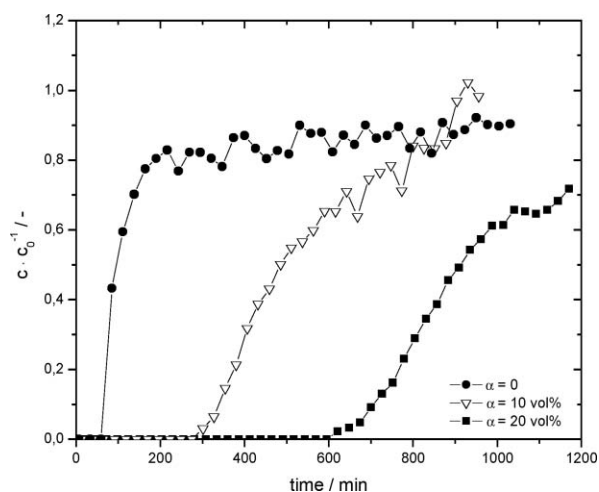


Fig. 6 Normalised breakthrough curves of n-butyl mercaptan with an unloaded support ($\alpha = 0$ vol%) and a $[\text{C}_{12}\text{MIM}]\text{Cl}/\text{SnCl}_2$ -based SILP material ($X = 0.50$) with different ionic liquid loadings; $T_{\text{abs}} \sim 90$ °C, $p = 1.05$ bar, $m_{\text{SILP}} = 10.6$ g, $h \sim 90$ mm, $V_{\text{N}_2} = 40$ Nml min^{-1} , $V_{\text{oil}} = 0.2$ ml min^{-1} .

Table 2 The saturation and breakthrough capacities, and breakthrough time of different SILP materials^a

Ad-/absorber filling	Metal content X	$x_b/\text{mg}_s \text{ g}_{\text{SILP}}^{-1}$	$x_s/\text{mg}_s \text{ g}_{\text{SILP}}^{-1}$	t_b/min
Al ₂ O ₃ support without ionic liquid	—	0.56	0.64	85
[C ₄ MIM]Cl/ZnCl ₂	0.50	0.37	0.53	62
[C ₄ MIM]Cl/SnCl ₂	0.50	1.35	2.37	216
[C ₈ MIM]Cl/SnCl ₂	0.50	2.48	3.97	395
[C ₁₂ MIM]Cl/SnCl ₂	0.33	0.88	0.98	145
[C ₁₂ MIM]Cl/SnCl ₂	0.50	3.90	5.76	621
[C ₁₂ MIM]Cl/SnCl ₂	0.57	1.84	2.70	296
[C ₁₂ MIM]Cl/SnCl ₂	0.62	1.27	1.97	185
[C ₁₂ MIM][Tf ₂ N]	—	0.26	0.38	41

^a SILP materials ($\alpha = 20 \text{ vol}\%$) with different molar ratios, X , of MCl₂; $T_{\text{abs}} \sim 90 \text{ }^\circ\text{C}$, $p = 1.05 \text{ bar}$, $m_{\text{SILP}} = 10.6 \text{ g}$, $h \sim 90 \text{ mm}$, $V_{\text{N}_2} = 40 \text{ Nml min}^{-1}$, $V_{\text{MO}} = 0.2 \text{ ml min}^{-1}$.

A clear correlation between the sorption performance of the tested SILP materials and the ionic liquid loading on the support was observed. Without ionic liquid, the breakthrough time was only 85 min. In contrast, the SILP material with $\alpha = 0.1$ removed all n-butyl mercaptan from the gas stream for 300 min time-on-stream. The almost proportional further increase of the breakthrough time to 620 min with $\alpha = 0.2$ indicates that there was no obvious detrimental influence of pore flooding to this ionic liquid loading. Pore flooding and blocking of transport pores would obviously reduce the degree of ionic liquid utilization in the system and would thus reduce the efficiency of gas sorption. Higher ionic liquid loadings were not feasible, since the ionic liquid film becomes mobile, and can be removed by gravity and convection under such conditions (e.g. 30 vol% ionic liquid and 90 °C). This would result in SILP materials with undefined properties, making it difficult to evaluate their extraction performance.

Stability and regeneration

So far, all of the reported results have been obtained in single pass experiments. It is obvious that for the practical industrial application of these SILP materials in gas cleaning processes appropriate regeneration is required to unload the SILP materials of S-compounds for the repetitive use of the SILP column.

In order to test this option, we applied a combined pressure and temperature swing for unloading and SILP material regeneration. The S-saturated SILP material was heated from 90 (sorption temperature) to 130 °C, while at the same time the pressure in the column was reduced to 2.5×10^{-2} mbar. These regeneration conditions were maintained for 3 h before sorption conditions were again applied for the next loading cycle. The results for four consecutive sorption/regeneration cycles are depicted in Fig. 7.

This experiment indeed proves the general suitability of the applied chlorostannate SILP material for repetitive loading and unloading cycles. However, the performance in S removal decreased from 830 min breakthrough time in the first cycle to 520 min in the fourth. Note that the breakthrough time in the first cycle exceeded the one we observed for the same SILP material in previous experiments (see for example Table 2 and Fig. 6). This notable difference was obviously caused by the thermal pre-treatment (120 °C, 2.5×10^{-2} mbar, 60 min) of the SILP material

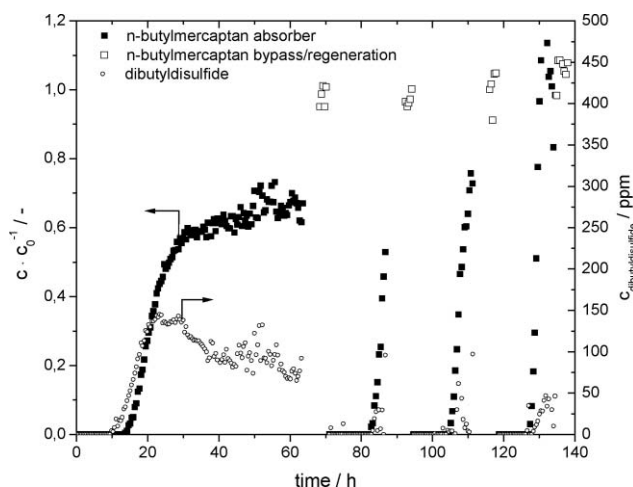


Fig. 7 Normalised breakthrough curves of n-butyl mercaptan in long-term experiments with regeneration; SILP material: [C₁₂MIM]Cl/SnCl₂ ($X = 0.50$) on alumina with $\alpha = 0.2$; $T_{\text{abs}} \sim 90 \text{ }^\circ\text{C}$, $p = 1.05 \text{ bar}$, $m_{\text{SILP}} = 10.6 \text{ g}$, $h \sim 90 \text{ mm}$, $V_{\text{N}_2} = 40 \text{ Nml min}^{-1}$, $V_{\text{oil}} = 0.2 \text{ ml min}^{-1}$; regeneration at $T_{\text{abs}} = 130 \text{ }^\circ\text{C}$ and $p = 2.5 \times 10^{-2}$ mbar for 180 min.

prior to the first loading cycle in the experiments displayed in Fig. 7. The reduction of sorption performance over several regeneration cycles is attributed to an incomplete removal of the adsorbed sulfur compounds from the ionic liquid during the regeneration procedure. In this context, it is important to notice that in the repetitive loading/unloading experiment, the GC analysis indicated the formation of dibutylsulfide. This product results from a condensation reaction of two molecules n-butyl mercaptan. The latter reaction is known to proceed at elevated temperatures ($>100 \text{ }^\circ\text{C}$) in the absence of any catalyst.²⁴ Our results suggest that the applied sorption conditions produced a relevant amount of this dibutylsulfide side-product. Due to the elevated boiling point of the latter (b.p. $> 220 \text{ }^\circ\text{C}$), it was obviously not possible to completely remove the dibutylsulfide from the SILP material by the applied regeneration procedure. Consequently, a SILP material of reduced capacity for n-butyl mercaptan sorption was obtained for the next cycle. For the further development of gas cleaning technologies by SILP sorption processes, it is therefore relevant to adapt the sorption conditions in a way that avoids the formation of heavy products that are difficult to remove in the regeneration cycle. Apart from this important optimization aspect, our results can be regarded as a successful proof of

principle for the application of SILP materials in pressure and temperature swing sorption processes for gas cleaning purposes.

Conclusions

This work describes for the first time the use of supported ionic liquid phase (SILP) materials in gas cleaning technologies. The system $[C_{12}MIM]Cl/SnCl_2$ ($X = 0.50$) on alumina (with an ionic liquid loading equal to 20% of the alumina pore volume) has proved to be particularly suitable for the removal of n-butyl mercaptan from n-heptane vapour. At a 90 °C sorption temperature and under atmospheric pressure, a total gas volume of 73 L containing 500 ppm_w n-butyl mercaptan was purified to below 5 ppm_w mercaptan using 10.6 g of SILP material. At a combined gas flow rate of 87.5 ml min⁻¹, breakthrough of the S-compound at the outlet of the sorption column was only observed after 830 min time-on-stream. More importantly, the regeneration of the SILP material could be demonstrated by applying a temperature and pressure swing. Four consecutive loading/unloading cycles were successfully demonstrated over a 130 h total operation time. Due to some formation of dibutyl disulfide during the sorption cycles, the capacity of the SILP material was found to decrease slowly from one cycle to the next. Obviously, removal of the higher boiling dibutyl disulfide was incomplete during the applied regeneration cycle. It is noteworthy, however, that in the fourth loading cycle, n-butyl mercaptan was still fully removed from the gas stream for more than 8 h time-on-stream. Avoiding the formation of dibutyl disulfide by lowering the absorption temperature should further increase the SILP sorber material operation time and regenerability.

We are convinced that our findings will excite further interest in the use of SILP materials for gas cleaning technologies. It is obvious that the specific property profiles offered by ionic liquids (e.g. extremely low volatility, tuneable solubility properties, compatibility with dissolved transition metal complexes for reversible gas complexation) fit in an ideal manner with the technical requirements of advanced materials for gas purification purposes. In addition to these general ionic liquid features, the use of the SILP concept offers a high gas/liquid exchange area, very efficient ionic liquid utilisation and short diffusion distances. Due to this highly attractive set of features, we are convinced that the use of SILP sorber materials will gain importance for a number of technically relevant gas purification processes in the near future. We anticipate interesting application scenarios, both for the removal of hazardous gas components from exhaust streams and for the purification of valuable gases in a highly energy efficient manner.

Acknowledgements

The authors thank Andreas Bösmann (TGA measurements), Natalia Paape (ionic liquid synthesis) and Martina Kormann

(support characterisation) for their contributions. Sasol Germany GmbH is acknowledged for the supply of alumina support. Financial support from the Deutsche Bundesstiftung Umwelt (DBU) and the Cluster of Excellence "Engineering of Advanced Material" is gratefully acknowledged.

References

- 1 EU directive 98/70/EC of the European Parliament and of the Council of 13 October 1998. Available at <http://eur-lex.europa.eu/LexUriServ/LexUriServ.do?uri=CELEX:31998L0070:EN:NOT> (accessed May 2010).
- 2 EPA-Diesel RIA, United States Environmental Protection Agency, Air and Radiation, EPA420-R-00-026, 17 May 2000. Available on <http://www.epa.gov/OMS/regs/fuels/diesel/epapress.pdf> (accessed March 2010).
- 3 K. G. Knudsen, B. H. Cooper and H. Topsøe, *Appl. Catal., A*, 1999, **189**, 205.
- 4 A. Bösmann, L. Datsevich, A. Jess, A. Lauter, C. Schmitz and P. Wasserscheid, *Chem. Commun.*, 2001, 2494.
- 5 S. Zhang, Q. Zhang and Z. C. Zhang, *Ind. Eng. Chem. Res.*, 2004, **43**, 614.
- 6 C. Huang, B. Chen, J. Zhang, Z. Liu and Y. Li, *Energy Fuels*, 2004, **18**, 1862.
- 7 Q. Dongjun, L. Jing and S. Li, *China Petroleum Process. Petrochem. Tech.*, 2009, **4**, 34.
- 8 N. Victorovna Likhanova, R. Martinez Palou, S. Palomeque, F. Jorge, *US Pat. Appl. Publ.*, US 2009288992, 2009, 7.
- 9 E. Kuhlmann, M. Haumann, A. Jess, A. Seeberger and P. Wasserscheid, *ChemSusChem*, 2009, **2**, 969.
- 10 H. Gao, Y. Li, Y. Wu, M. Luo, Q. Li, J. Xing and H. Liu, *Energy Fuels*, 2009, **23**, 2690.
- 11 J. Eßer, P. Wasserscheid and A. Jess, *Green Chem.*, 2004, **6**, 316.
- 12 A. Riisager, R. Fehrmann, M. Haumann and P. Wasserscheid, *Top. Catal.*, 2006, **40**, 91.
- 13 <http://www.silp-technology.de> (accessed 1 April 2010).
- 14 S. Werner, N. Szesni, A. Bittermann, M. J. Schneider, P. Haerter, M. Haumann and P. Wasserscheid, *Appl. Catal., A*, 2010, **377**, 70.
- 15 J. Joni, M. Haumann and P. Wasserscheid, *Appl. Catal., A*, 2010, **372**, 8.
- 16 M. Haumann, K. Dentler, J. Joni, A. Riisager and P. Wasserscheid, *Adv. Synth. Catal.*, 2007, **349**, 425.
- 17 A. Riisager, R. Fehrmann, M. Haumann and P. Wasserscheid, *Eur. J. Inorg. Chem.*, 2006, 695.
- 18 A. Riisager, R. Fehrmann, M. Haumann, B. S. K. Gorle and P. Wasserscheid, *Ind. Eng. Chem. Res.*, 2005, **44**, 9853.
- 19 C. J. Bowles, D. W. Bruce and K. R. Seddon, *Chem. Commun.*, 1996, 1625.
- 20 L. Carson, P. K. W. Chau, M. J. Earle, M. A. Gilea, B. F. Gilmore, S. P. Gorman, M. T. McCann and K. R. Seddon, *Green Chem.*, 2009, **11**, 492.
- 21 K. R. J. Lovelock, C. Kolbeck, T. Cremer, N. Paape, P. S. Schulz, P. Wasserscheid, F. Maier and H. -P. Steinrück, *J. Phys. Chem. B*, 2009, **113**, 2854.
- 22 N. H. Ko, J. S. Lee, E. S. Huh, H. Lee, K. D. Jung, H. S. Kim and M. Cheong, *Energy Fuels*, 2008, **22**, 1687.
- 23 (a) K. S. Hwang and W. K. Lee, *Sep. Sci. Technol.*, 1994, **29**, 1857; (b) J. Tantet, M. Eić and R. Desai, *Gas Sep. Purif.*, 1995, **9**, 213.
- 24 M. Kirihara, Y. Asai, S. Ogawa, T. Noguchi, A. Hatano and Y. Hirai, *Synthesis*, 2007, 3286.